Available online at www.sciencedirect.com

ScienceDirect

Physica C 468 (2008) 337–340

PHYSICA C

www.elsevier.com/locate/physc

Quantum phase transition in ultra small doubly connected superconducting cylinders

I. Sternfeld [a,*], R. Koret [a], H. Shtrikman [b], A. Tsukernik [c], M. Karpovski [a], A. Palevski [a]

[a] School of Physics and Astronomy, Raymond and Beverly Sackler Faculty of Exact Sciences, Tel Aviv University, Tel Aviv 69978, Israel
[b] Department of Condensed Matter, Weizmann Institute of Science, Rehovot 76100, Israel
[c] The Center for Nanoscience and Nanotechnology, Tel Aviv University, Tel Aviv 69978, Israel

Accepted 4 August 2007
Available online 6 November 2007

Abstract

The kinetic energy of Cooper pairs, in doubly connected superconducting cylinders, is a function of the applied flux and the ratio between the diameter of the cylinder and the zero temperature coherence length $d/\xi(0)$. If $d > \xi(0)$ the known Little–Parks oscillations are observed. On the other hand if $d < \xi(0)$, the superconducting state is energetically not favored around odd multiples of half flux quanta even at $T \sim 0$, resulting in the so called destructive regime [Y. Liu, et al., Science 294 (2001) 2332]. We developed a novel technique to fabricate superconducting doubly connected nanocylinders with both diameter and thickness less than 100 nm, and performed magnetoresistance measurements on such Nb and Al cylinders. In the Nb cylinders, where $d > \xi(0)$, we observed the LP oscillations. In the Al cylinders we did not observe a transition to the superconducting state due to the proximity effect, resulted from an Au layer coating the Al. However, we did observe Altshuler–Aronov–Spivak (h/2e) oscillations in these cylinders.

PACS: 74.78.Na; 74.78.−w; 73.43.Nq; 68.70.+w

Keywords: Superconductivity; Quantum phase transition

1. Introduction

Quantum phase transitions (QPT) is an active topic in modern solid-state physics [2,3]. An important and interesting example for such transitions is the superconductor–insulator [3–8] QPT. In this case, external parameters such as disorder [2,5], pressure [6] or applied magnetic field [7,8] force the superconductor quantum ground state to transit into a fundamentally different ground state. Some studies indicate that when superconductivity is destroyed, an anomalous finite resistance metallic phase emerges rather than the predicted insulating state [4]. Currently, the subject remains unresolved and highly controversial [4,9,10], to a large extent due to lack of clear cut experimental findings.

Recently, it was demonstrated [1] that superconductivity can also be suppressed, in a rather unique manner in a doubly connected superconducting cylinder with diameter d, which is shorter than the zero temperature superconductor coherence length $\xi(0)$. When odd multiples of half flux quanta thread such a system, the superconducting state is energetically not favored even at $T \simeq 0$, resulting in the so called destructive regime, which can be used as a powerful tool for studying QPT.

The physics of the destructive regime is intimately related to the well-known phenomenon of Little–Parks (LP) oscillations of the critical temperature (T_C) versus magnetic flux, Φ [11]. These oscillations are due to competition between the condensation energy and the kinetic energy of the Copper pairs. In a sufficiently thin-walled superconductor hollow cylinder the Copper pairs velocity, v_s, is a periodic function of the external magnetic flux [12]:

* Corresponding author.
E-mail address: itayst@post.tau.ac.il (I. Sternfeld).

0921-4534/$ - see front matter © 2007 Elsevier B.V. All rights reserved.
doi:10.1016/j.physc.2007.08.024

$$v_s = \frac{2\hbar}{m^* d}\left(n - \frac{\Phi}{\Phi_0}\right). \tag{1}$$

Here, m^* is the Cooper pairs' mass, $\Phi_0 = \frac{hc}{e^*}$ is the flux quantum and the integer n minimizes the superconducting current, thus allowing the system to remain in the superconducting state at the highest possible temperature. When the flux through the cylinder is increased v_s is increased as well, leading to a reduction in T_C, given by [12]:

$$\frac{T_C(0) - T_C(H)}{T_C(0)} = \left\{ \begin{array}{ll} 2.2\frac{\xi_0^2}{d^2}(n - \frac{\Phi}{\Phi_0})^2 & \text{clean limit} \\ 2.92\frac{\xi_0 l}{d^2}(n - \frac{\Phi}{\Phi_0})^2 & \text{dirty limit} \end{array} \right\} \tag{2}$$

Here ξ_0 is the BCS coherence length and l is the mean free path. When $\Phi = n\Phi_0$, there are no screening currents and there is no depression of T_C. On the other hand, when $\Phi = (n + \frac{1}{2})\Phi_0$, the screening currents attain their maximum value and T_C its minimum one. Experimentally, the LP effect can be observed as a periodic variation of the resistance of a cylinder (or ring) with magnetic field, at a fixed temperature around the middle of the normal-superconducting transition.

From Eq. (2) it is obvious that the depression of T_C depends on the ratio $\xi(0)/d$. Indeed, most previous experiments were done using cylinders or rings having $\xi(0)/d \ll 1$ and, therefore, the observed oscillations never exceeded a few percents. However, the technological advances in submicron fabrication enable to approach the limit where the diameter of the cylinder could be smaller than the coherence length. In this case, $T_C = 0$ in some vicinity of $\Phi/\Phi_0 = n + \frac{1}{2}$. There is a critical flux Φ_C, such that at fluxes $\Phi = n\Phi_0 \pm \Phi_C$, there is a superconductor–nonsuperconductor phase transition, at $T = 0$. Φ_C can be obtained from the Ginzburg–Landau expression for the order parameter of a thin superconducting film, in the presence of magnetic field [12], $|\Psi|^2 \propto [1 - (\frac{\xi(T)m^* v_s}{\hbar})^2]$ and Eq. (1):

$$\Phi_C = \frac{d\Phi_0}{2\xi(T)} \tag{3}$$

In the dirty limit this yields $\Phi_C = 0.58\frac{d\Phi_0}{\sqrt{\xi(0)l}}$. Vafek *et al.* [9] calculated Φ_C using mean field theory and obtained $\Phi_C = 0.49\frac{d\Phi_0}{\sqrt{\xi(0)l}}$.

Liu et al. [1,14] succeeded in fabricating Al and $Au_{0.7}In_{0.3}$ cylinders of 150 nm diameter with a zero temperature coherence length, ξ_0 in the range of 100–200 nm. In spite of the fact that the condition $d < \xi_0$ was barely met in the experiment, the vanishing T_C was clearly observed near $\frac{\Phi}{\Phi_0} = \frac{1}{2}, \frac{3}{2}$. Furthermore, the value of Φ_C was in good agreement with the theoretical predictions stated above.

2. Experimental

Sample fabrication of superconducting doubly connected nanocylinders consists of three major steps: molecular beam epitaxy (MBE) growth of GaAs nanowire, deposition of a superconducting coating film, and nano fabrication of electrical leads.

A standard Riber 32 solid source growth system is used for the growth of high quality GaAs nanowires by the well established vapor–liquid–solid (VLS) technique [15–17]. Nano size Au particles covering the substrate serve as nano size solutions which transfer Ga and As impinging on the sample into the growth interface. The diameter of the Au droplets and the growth time determine the wires diameter and length, respectively.

For MBE growth of GaAs nanowires, a one nanometer thick Au layer was evaporated on an etched GaAs <1 1 1>B substrate in an external evaporator and quickly loaded into the MBE system. After outgassing in a separate chamber, the sample was transferred into the growth chamber where it was heated above the eutectic temperature of Au and GaAs producing randomly distributed Au droplets of different diameters. Growth temperature for GaAs nanowires is 550 °C and the Ga to As flux ratio on the order of 1:100 to assure fair competition between wires growth and bulk growth in the vicinity of the Au droplets. The Au droplets are considered to be the catalysts for the growth of nanowires. Growth occurs at the interface of the Au droplet and the surface, where the Au droplet remains floating at the top of the growing wire. The GaAs wires normally assume the Wurtzite hexagonal structure, having occasional stalking faults related to the occurrence of the Zinc Blende structure as we learn from TEM (transmission electron microscope). The single crystal nanowires are typically 2–5μm long and 40–50 nm or 70–90 nm in diameter, as we can see from the high resolution scanning electron microscope (HR-SEM) images.

The grown nanowires are used as a mold for the deposition of a superconducting film. Nb or Al are sputtered on the substrate with a Pfeiffer PLS 160 sputtering system. The thickness of the film deposited on the nanowires is determined by the sputtering time. The superconducting films are *in situ* covered by a thermally evaporated Au layer in order to prevent oxidation and enable good electrical contact to the superconducting layer. The total diameter

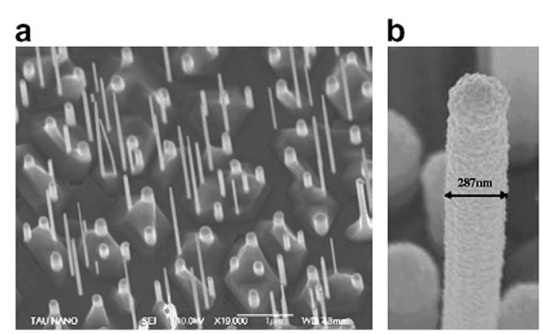

Fig. 1. HRSEM micrograph of: (a) Typical 70–90 nm diameter GaAs nanowires. (b) A nanowire covered with Al and Au. The thickness of the Al layer is about 60 nm and the total diameter of the nanowire is approximately 290 nm.

of the nanowire, which is about 250 nm, is estimated later using an HR-SEM, as can be seen in Fig. 1.

The nanowires covered by a superconductor are pressed against a blank silicon oxide wafer covered by PMMA (e-beam lithography resist) thus leaving a large number of nanowires aligned parallel to the surface. The wires are covered by an additional PMMA layer to prevent carbon contamination in the proceeding selection procedure. Appropriate nanowires are selected and pinned to the wafer by long exposure to the HR-SEM electron beam, which hardens the PMMA. The remaining (undesired) nanowires are washed away with acetone. In order to enable contact between the superconducting nanowire and the future metallic contacts, a low-pressure oxygen plasma is used to etch the hardened PMMA, which covers the nanowires upper surface. A standard lift off e-beam lithography technique is employed. Ti (10 nm) and 60 nm of Au are deposited by an electron beam gun vacuum evaporator. A typical result of this process is presented in Fig. 2. The sample is manually aligned and bonded to a socket sample holder, so that the nanowire is parallel to the socket's edge and to the applied magnetic field. The sample is bonded to the socket pads using an MEI 1204 W Hybrid Wedge Bonder, with aluminum wires. The resistance was measured by a four-terminal method using a low noise analog lock-in amplifier (EG&G PR-124A) in a dilution refrigerator or a ^{4}He cryogenic system.

3. Results and discussion

We have performed magnetoresistance measurements of Nb coated nanowires fabricated as described above. The normal metal–superconductor phase transition is broad, 2–6 K. $R_N = 40\ \Omega$ is the normal state resistance, and the resistivity is $3.4 * 10^{-3}\ \Omega$ cm. $T_C = 2.26$ K, is defined here as the temperature at which $R = R_N/10 = 4\ \Omega$. The normalized resistance as a function of the flux threading the cylinder is presented in Fig. 3. This measurement was done just below the critical temperature at $T = 2.18$ K. The LP oscillations are accompanied by a quadratic background term, which is related to misalignments between the cylinder and the magnetic field [12] and to the finite thickness of the superconducting wall. Using the oscillations period, $\Delta H = 600$ G, and $\Phi_0 = \frac{1}{4}\pi d^2 \Delta H$, we deduced that the cylinders diameter is $d \approx 200$ nm, which is in reasonable agreement with the HRSEM observations (see Fig. 1). The error in this measurement is about 5%. Using the data presented in Fig. 3 and the data of R vs. T with $H = 0$, we constructed a plot of $\Delta T_C/T_C$ as a function of the flux (see Fig. 4). The maximum relative degradation of T_C is $\Delta T_C/T_C = 0.025$. Even though this measurement was conducted on Nb, which has a short coherence length ($\xi_0 = 38$ nm [18]), the depression of T_C is an order of magnitude larger than the depression observed by Little and Parks [11] in their original work on a Sn ($\xi_0 = 250$ nm [18]) cylinder of about 1400 nm in diameter.

We also performed low temperature transport measurements of Al coated nanowires fabricated as described above, and did not observe a phase transition into the superconducting phase. It could be that the Au protective layer in this sample was thick enough to suppress superconductivity by the proximity effect. Magnetoresistance measurements of this sample are presented in Fig. 5 for three different temperatures. We presume that the observed oscillations are

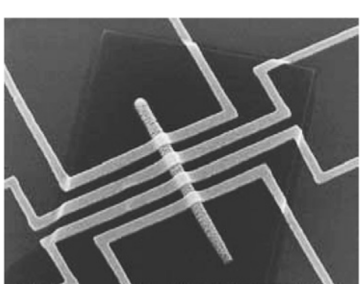

Fig. 2. HRSEM micrograph of an Al–Au nanowire with ohmic contacts. The dark area surrounding the nanowire is the hardened PMMA.

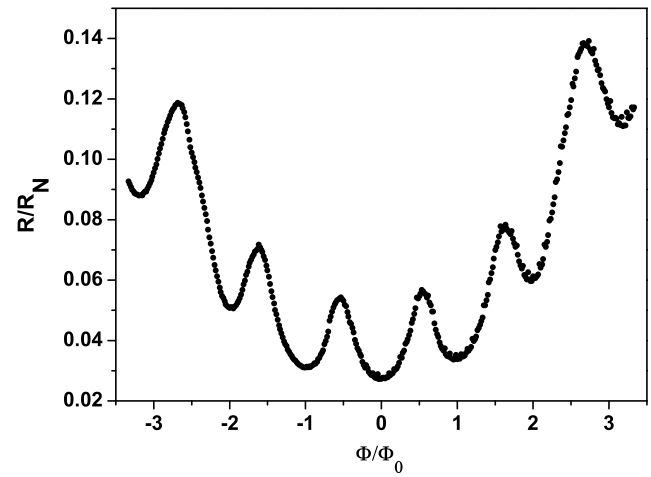

Fig. 3. Resistance as a function of applied flux in Nb doubly connected nanocylinder, in which LP oscillations are observed. The measurement is conducted just below T_C, at $T = 2.18$ K, with $I = 1$ μA.

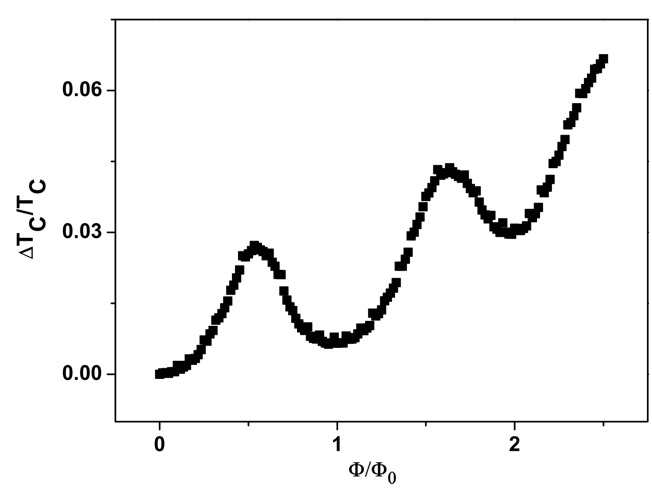

Fig. 4. $\Delta T_C/T_C$ as a function of the flux in Nb doubly connected nanocylinder.

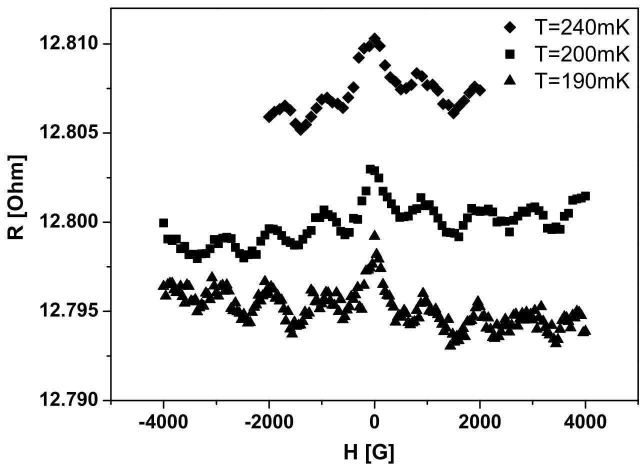

Fig. 5. Resistance as a function of applied field in Al doubly connected nanocylinder at three different temperatures, in which the AAS oscillations are observed.

Al'tshuler–Aronov–Spivak (AAS) h/2e oscillations [19]. Fourier transform analysis verified that there is only one frequency with $\Delta H = 950\,\mathrm{G}$, which corresponds to $d \approx 165$ nm.

Since the amplitude of the oscillations is small, $\frac{\Delta R}{R} = 10^{-4}$, a relatively high current of 1 μA and long time constant in the lock-in were needed to improve signal to noise ratio. Our measurements show negative zero field magnetoresistance. It is known [20] that the presence of Au particles causes positive zero field magnetoresistance due to spin orbit interaction. It is possible that the negative zero field magneto resistance indicates that the electrons path is mostly in the Al rather than in the Au.

4. Summary

In summary we presented a novel technique to fabricate nano size superconducting doubly connected cylinders. LP oscillations were observed on such Nb cylinders. To the best of our knowledge, these are the smallest cylinders in which the phenomenon was demonstrated. The presented results indicate that this technique is suitable for the study of the destructive regime and QPT.

Acknowledgements

The support of the Israel Science Foundation founded by the Israel Academy of Sciences and Humanities, Centers of Excellence Program is gratefully acknowledged.

References

[1] Y. Liu et al., Science 294 (2001) 2332.
[2] S.L. Sondhi et al., Rev. Mod. Phys. 69 (1997) 315.
[3] T. Vojta, Annalen der Physik 9 (2000) 403.
[4] A. Kapitulnik et al., Phys. Rev. B 63 (2001) 125322.
[5] S. Chakravarty, B.I. Halperin, D. Nelson, Phys. Rev. Lett. 60 (1988) 1057;
S. Chakravarty, B.I. Halperin, D. Nelson, Phys. Rev. B 39 (1989) 2344.
[6] V.P. Mineev, M. Sigrist, Phys. Rev. B 63 (2001) 172504.
[7] S. Sachdev, Quantum Phase Transitions, Cambridge University Press, Cambridge, 2000, and references therein.
[8] Y. Liu et al., Phys. Rev. B 47 (1993) 5931.
[9] O. Vafek, M.R. Beasley, S. Kivelson, cond-mat/0505688 (2005).
[10] P. Phillips, D. Dalidovich, Science 302 (2003) 243.
[11] W. Little, R. Parks, Phys. Rev. Lett. 9 (1962) 9.
[12] M. Tinkham, Introduction to Superconductivity, McGraw Hill, 1996.
[14] H. Wang et al., Phys. Rev. Lett. 95 (2005) 197003.
[15] L.E. Jensen et al., Nano Lett. 4 (2004) 1961.
[16] Y. Wu et al., Nature 430 (2004) 61;
X. Duan et al., Nature 409 (2001) 66.
[17] K.A. Dick et al., Nano Lett. 4 (2005) 761.
[18] T. Van Duzer, C.W. Turner, Principles of Superconductive Devices & Circuits, Elsevier, New York, 1981.
[19] A.G. Aronov, Yu. V. Sharvin, Rev. Mod. Phys. 59 (1987) 755.
[20] G. Bergmann, Phys. Rev. Lett. 48 (1982) 1046.